Am J Stem Cells 2026;15(1):1-12
www.AJSC.us /ISSN:2160-4150/AJSC0168187

Original Article

GDF11 activates AMPK-dependent mitophagy to drive osteogenic differentiation of rat bone marrow mesenchymal stem cells

Xinfeng Gao, Qiting He, Junjun Chen, Gen Wu, Shaoqiang Xia, Shuaiwei Shang, Linghang Xue, Xinqiang Bei, Kai Xiao

Department of Orthopedic Surgery, Wuhan Fourth Hospital, Wuhan 430030, Hubei, China

Received August 18, 2025; Accepted December 2, 2025; Epub February 15, 2026; Published February 28, 2026

Abstract: Background: Growth differentiation factor 11 (GDF11) has emerged as a potential regulator of bone regeneration; however, the molecular mechanisms through which it influences osteogenic differentiation, particularly in relation to mitochondrial quality control, remain unclear. This study aimed to elucidate the role of adenosine monophosphate-activated protein kinase (AMPK)-dependent mitophagy in GDF11-mediated osteogenic differentiation of rat bone marrow mesenchymal stem cells (rBMMSCs). Methods: rBMMSCs were induced toward osteogenic differentiation with or without GDF11 treatment. To specifically inhibit AMPK-dependent mitophagy, Compound C, an AMPK inhibitor, was employed. Osteogenic differentiation was evaluated using alkaline phosphatase (ALP) staining and activity assays, while Alizarin Red S (ARS) staining was performed to assess matrix mineralization. The expression of Mitophagy- and osteogenesis-associated markers was analyzed through immunofluorescence staining, quantitative real-time PCR, and western blotting. Results: GDF11 significantly enhanced the osteogenic differentiation of rBMMSCs, as evidenced by increased ALP activity, more intense ALP staining, enhanced calcium nodule formation, and elevated expression of ALP and RUNX2. GDF11 activated mitochondrial function by promoting AMPK phosphorylation and inducing Mitophagy. Inhibition of AMPK significantly impaired Mitophagy, while Compound C-mediated blockade of AMPK-dependent mitophagy not only suppressed basal osteogenic differentiation but also abolished the pro-osteogenic effects of GDF11. This was reflected by a pronounced reduction in GDF11-induced ALP activity, mineralization, and the expression of key osteogenic genes at both the mRNA and protein levels. Conclusion: GDF11 enhances the osteogenic differentiation of rBMMSCs by activating AMPK-dependent mitophagy. These findings identify AMPK-dependent Mitophagy as a pivotal mechanism mediating the osteogenic actions of GDF11, providing new mechanistic insights that may guide the development of novel strategies for bone regeneration.

Keywords: Growth differentiation factor 11, AMPK, mitophagy, osteogenic differentiation, bone marrow mesenchymal stem cells

Introduction

Osteoporosis (OP) is a systemic skeletal disorder characterized by a significant reduction in bone mass and deterioration of bone microarchitecture, which constitutes the primary pathological basis for the increased fracture risk observed in the elderly population [1]. Affecting more than 200 million individuals worldwide, OP leads to severe clinical consequences; hip fractures alone carry an alarming 1-year mortality rate of up to 20%, placing a heavy burden on patients, their families, and healthcare systems [2]. Current clinical treatments primarily aim to inhibit bone resorption (e.g., bisphosphonates) or stimulate bone formation (e.g., teriparatide) [3]. However, these strategies are limited by adverse effects, high treatment costs, and inconsistent long-term efficacy, underscoring the need to identify novel molecular targets and therapeutic approaches for regulating bone metabolism.

Bone marrow mesenchymal stem cells (BMMSCs), the main precursors of osteoblasts, possess robust osteogenic potential and play a central role in maintaining skeletal homeostasis [4]. In the osteoporotic microenvironment, however, the osteogenic differentiation capacity of BMMSCs is significantly impaired, while

https://doi.org/10.62347/RLSG3699

their susceptibility to apoptosis increases [5]. This imbalance leads to reduced bone formation and accelerated bone loss. Recent evidence highlights the pivotal contribution of organelle homeostasis, particularly mitochondrial function, in determining stem cell fate [6]. Mitophagy, a specialized form of autophagy responsible for eliminating damaged mitochondria, is crucial for maintaining cellular energy metabolism and redox balance. Its activity directly influences the differentiation potential of stem cells, including BMMSCs [7]. The accumulation of dysfunctional mitochondria triggers excessive production of reactive oxygen species (ROS) and bioenergetic deficits, severely compromising osteogenic differentiation [8]. Activation of Mitophagy has been shown to enhance the osteogenic capacity of BMMSCs. Therefore, understanding the molecular regulators and mechanisms that control Mitophagy in BMMSCs is essential for elucidating the cellular basis of OP and developing new therapeutic approaches.

Growth differentiation factor 11 (GDF11), a member of the transforming growth factor-β (TGF-β) superfamily, has garnered significant attention due to its diverse biological roles, particularly in aging and tissue regeneration [9]. Despite ongoing debate over its proposed anti-aging properties, multiple studies have confirmed the positive regulatory role of GDF11 in bone metabolism [10]. Administration of exogenous GDF11 has been shown to ameliorate osteoporosis induced by ovariectomy or aging, significantly improving bone mass and mechanical strength [11]. However, the downstream signaling pathways through which GDF11 promotes osteogenesis in BMMSCs, especially those involving mitochondrial quality control, remain poorly understood.

Adenosine monophosphate-activated protein kinase (AMPK) acts as a central sensor and regulator of cellular energy metabolism. It is activated under conditions of energy stress, such as increased AMP/ATP ratios, through the phosphorylation of its Thr172 residue by upstream kinases, including LKB1 [12]. AMPK plays a crucial role in regulating glucose and lipid metabolism, as well as maintaining mitochondrial homeostasis [13]. It can positively regulate Mitophagy either through direct phosphorylation of autophagy-initiating proteins such as ULK1 or *via* transcriptional modulation of mitophagy-related genes [14]. Emerging evidence indicates that GDF11 may activate AMPK signaling in specific cell types [15]. This raises a key mechanistic question: Does GDF11 promote the osteogenic differentiation of BMMSCs through AMPK activation and subsequent enhancement of Mitophagy? Moreover, could dysregulation of this pathway contribute to the pathogenesis of OP? To date, these questions remain largely unanswered.

Based on these observations, the present study aimed to elucidate the mechanism by which GDF11 regulates the osteogenic differentiation of BMMSCs in the context of OP, focusing on the potential involvement of a "GDF11-AMPK phosphorylation-mitophagy" signaling axis. Primary rat BMMSCs were isolated and cultured *in vitro*, and a combination of genetic and pharmacological approaches, including lentivirus-mediated GDF11 overexpression and AMPK inhibition using Compound C, was employed. AMPK activation (Thr172 phosphorylation), mitophagy markers (e.g., PINK1), and osteogenic differentiation indicators (alkaline phosphatase [ALP] staining/activity, Alizarin Red S [ARS] staining, and the expression of RunX2 and ALP) were comprehensively analyzed. It is hypothesized that GDF11 enhances osteogenic differentiation by promoting AMPK phosphorylation and Mitophagy, improving mitochondrial function, and alleviating osteoporotic phenotypes. This study provides new insights into the molecular network underlying bone metabolism, identifies mitochondrial quality control as a critical regulatory node, and offers a theoretical foundation for developing innovative therapeutic strategies targeting the GDF11-AMPK-mitophagy axis in OP.

Materials and methods

Ethics statement

All animal experiments were conducted in accordance with the *Guidelines for the Care and Use of Laboratory Animals* and were approved by the Animal Ethics Committee of Wuhan Fourth Hospital. Sprague-Dawley (SD) rats were procured from SPF Biotechnology Co., Ltd. (Beijing, China).

Isolation and culture of primary rBMMSCs

Primary rBMMSCs were isolated from 6-week-old male SD rats weighing 100-150 g using the

whole bone marrow flushing method. The procedure was performed as follows: (1) Rats were euthanized *via* intraperitoneal injection of pentobarbital sodium (35 mg/kg), followed by cervical dislocation to ensure death. (2) The carcasses were sterilized by immersion in 75% ethanol for 15 minutes. (3) Femurs and tibias were aseptically excised, the surrounding muscle tissues were carefully removed, and the bones were rinsed with sterile phosphate-buffered saline (PBS; Beijing Dingguo Changsheng Biotechnology, China). (4) Both epiphyses were trimmed to expose the marrow cavities. (5) Bone marrow was flushed bidirectionally three times per bone into a 100-mm sterile culture dish (Nest, China) using Dulbecco's Modified Eagle Medium (DMEM; Gibco, USA) supplemented with 10% fetal bovine serum (FBS; Gibco, USA) and 1% penicillin-streptomycin (Gibco, USA). (6) The collected cell suspension was centrifuged at 1000 rpm for 5 minutes, the supernatant was discarded, and the pellet was resuspended in complete culture medium. (7) Cells were plated in 100-mm culture dishes (Nest) and incubated at 37°C in a humidified atmosphere containing 5% CO_2. (8) Non-adherent cells were removed after 48-72 hours by replacing the medium, which was subsequently refreshed every 3 days. (9) When cultures reached 80%-90% confluence, adherent cells were detached by trypsinization and subcultured at a 1:3 ratio.

Cells from passages 3 to 5 were used for all subsequent experiments.

ALP staining

The rBMMSCs were seeded in 12-well culture plates (Nest, China) at a density of 1×10^5 cells per well and cultured for 7 days in osteogenic differentiation medium (ODM). The ODM consisted of basal medium supplemented with 10% of FBS, 10 nM dexamethasone (Sigma Aldrich, USA), 5 mM β-glycerophosphate (Sigma Aldrich, USA), and 50 μg/mL ascorbate-2-phosphate (Sigma). The medium was replaced every 3 days.

After 7 days of induction, cells were processed as follows: (1) Washed three times with phosphate-buffered saline (PBS). (2) Fixed with 4% paraformaldehyde (Solarbio Life Sciences, Beijing, China) for 20 minutes at room temperature. (3) Washed three additional times with PBS. (4) Stained for alkaline phosphatase (ALP) activity using a BCIP/NBT color development kit (Beyotime, Shanghai, China) according to the manufacturer's instructions. (5) The stained cells were examined and imaged under a light microscope.

Measurement of ALP activity

The rBMMSCs were seeded in 12-well plates at a density of 1×10^5 cells per well. After 24 hours, the growth medium was replaced with osteogenic ODM, which was renewed every 3 days. On day 7, the following procedure was performed: (1) Cells were lysed using cell lysis buffer (Beyotime, China), homogenized, and centrifuged to collect the supernatant. Aliquots of the lysate (50 μL) were incubated with the substrate p-nitrophenyl phosphate at 37°C for 30 minutes using an ALP activity assay kit (Nanjing Jiancheng Bioengineering Institute, China). (2) The enzymatic activity of ALP was determined by measuring the absorbance at 405 nm with a microplate reader (Organon Teknika® Microwell Systems, USA). (3) Total protein concentration was quantified using a BCA protein assay kit (TaKaRa, Japan).

ALP activity was normalized to total protein content for subsequent analysis.

Alizarin Red S staining

Mineralized matrix formation was evaluated using Alizarin Red S (ARS) staining (Sigma-Aldrich, USA). rBMMSCs were seeded in 12-well plates at a density of 1×10^5 cells per well and cultured in osteogenic differentiation medium (ODM) for 14 days, with the medium refreshed every 3 days.

Staining procedure: (1) On day 14, cells were gently washed three times with PBS. (2) Cells were fixed with 4% paraformaldehyde (Sigma-Aldrich) for 10 minutes at room temperature, followed by three washes in PBS. (3) Each well was then incubated with 1% ARS solution (500 μL/well) for 30 minutes at room temperature. (4) After staining, cells were washed three times with PBS to remove excess dye. (5) The stained mineralized nodules were observed and photographed under a light microscope.

Quantification of mineralization: (1) Dye Elution: To extract bound ARS, 1 mL of 10% acetic acid (Beyotime, China) was added to each stained

Table 1. Sequences of primers

Gene	Forward (5'-3')	Reverse (5'-3')
ALP	AGATGGATGAGGCCATCGGA	CCAAACGTGAAAACGTGGGA
RUNX2	CAGACCAGCAGCACTCCATA	AGACTCATCCATTCTGCCGC
PINK1	TGCGCCAGTACCTTGAAGAG	TGAGGTCTCGATGGGCAATG
β-actin	CTCTGTGTGGATTGGTGGCT	CGCAGCTCAGTAACAGTCCG

well and incubated for 30 minutes at room temperature with gentle shaking. The cell layer was scraped to detach the matrix, and the resulting suspension was transferred to a 1.5 mL microcentrifuge tube. (2) Neutralization and Clarification: Tubes were vortexed for 30 seconds and then centrifuged at 20,000 × g for 15 minutes to pellet debris. A 500 µL aliquot of the supernatant was transferred to a new tube and neutralized by adding 200 µL of 10% ammonium hydroxide (Beyotime). (3) Spectrophotometric Measurement: Aliquots (100 µL per sample) were transferred to a 96-well plate, and the absorbance was measured at 405 nm using a microplate reader (Organon Teknika® Microwell Systems, USA).

Immunofluorescence (IF) staining

The rBMMSCs were seeded at a density of 5 × 10^4 cells per well onto ethanol-sterilized glass coverslips (Ø 14 mm; Nest, China) placed in 24-well plates (Nest) containing 500 µL of basal medium per well. When cells reached approximately 60%-70% confluence, the culture medium was replaced with ODM, and the cells were maintained for 3 days.

Staining procedure: (1) Cells were washed three times with PBS. (2) Fixed with 4% paraformaldehyde for 20 minutes at room temperature. (3) Washed three times with PBS. (4) Permeabilized with 0.2% Triton X-100 (Solarbio Life Sciences, Beijing, China) in PBS for 20 minutes at room temperature. (5) Washed three times with PBS. (6) Blocked with 5% bovine serum albumin (BSA; Solarbio Life Sciences, China) for 30 minutes at room temperature. (7) Incubated overnight at 4°C in a humidified chamber with a primary antibody against RUNX2 (1:200; ab76956, Abcam, USA). (8) Washed three times with PBS. (9) Incubated with TRITC-conjugated goat anti-mouse IgG secondary antibody (1:50; ZSGB-BIO, Beijing, China) for 1 hour at room temperature in the dark. (10) Washed three times with PBS. (11) Nuclei were counterstained with DAPI (Beyotime, China) for 5 minutes in the dark.

Imaging and quantification: Coverslips were mounted and imaged using a Lionheart FX fluorescence microscope (Bio-Tek, USA). RUNX2 fluorescence intensity was quantified in at least six randomly selected cells per condition using ImageJ software (NIH, USA), and the mean optical density values were used to represent relative protein expression levels.

RNA extraction and quantitative real-time PCR (qRT-PCR)

Total RNA was extracted from rBMMSCs on day 3 using TRIzol® reagent (Invitrogen, USA) according to the manufacturer's instructions. Complementary DNA (cDNA) was synthesized from the isolated RNA using a RevertAid™ First Strand cDNA Synthesis Kit (Fermentas, Canada). Quantitative PCR was subsequently performed with SYBR Green Master Mix (Takara, Japan) on an ABI 7300 Real-Time PCR System (Applied Biosystems, USA).

Primer sequences for the target genes *RUNX2*, *ALP*, and *PINK1*, as well as for the internal reference gene β-*actin*, are listed in **Table 1**. All primers were synthesized by Generay Biotechnology (Shanghai, China). Relative gene expression levels were normalized to β-actin and calculated using the $2^{-\Delta\Delta Ct}$ method.

Western blotting analysis

Cells were lysed in RIPA buffer (Sigma, USA) supplemented with a protease inhibitor cocktail (Roche, Switzerland). Total protein concentration was determined using a BCA protein assay kit (Takara, Japan). Equal amounts of protein were separated by 10% sodium dodecyl sulfate-polyacrylamide gel electrophoresis (SDS-PAGE) and subsequently transferred onto polyvinylidene fluoride (PVDF) membranes.

Immunoblotting procedure: (1) Membranes were blocked with 5% skim milk in Tris-buffered saline containing 0.1% Tween-20 (TBST) for 2 hours at room temperature. (2) Membranes were then incubated overnight at 4°C with the following primary antibodies: RUNX2 (1:1000, ab76956, Abcam, UK), ALP (1:1000, ab224335,

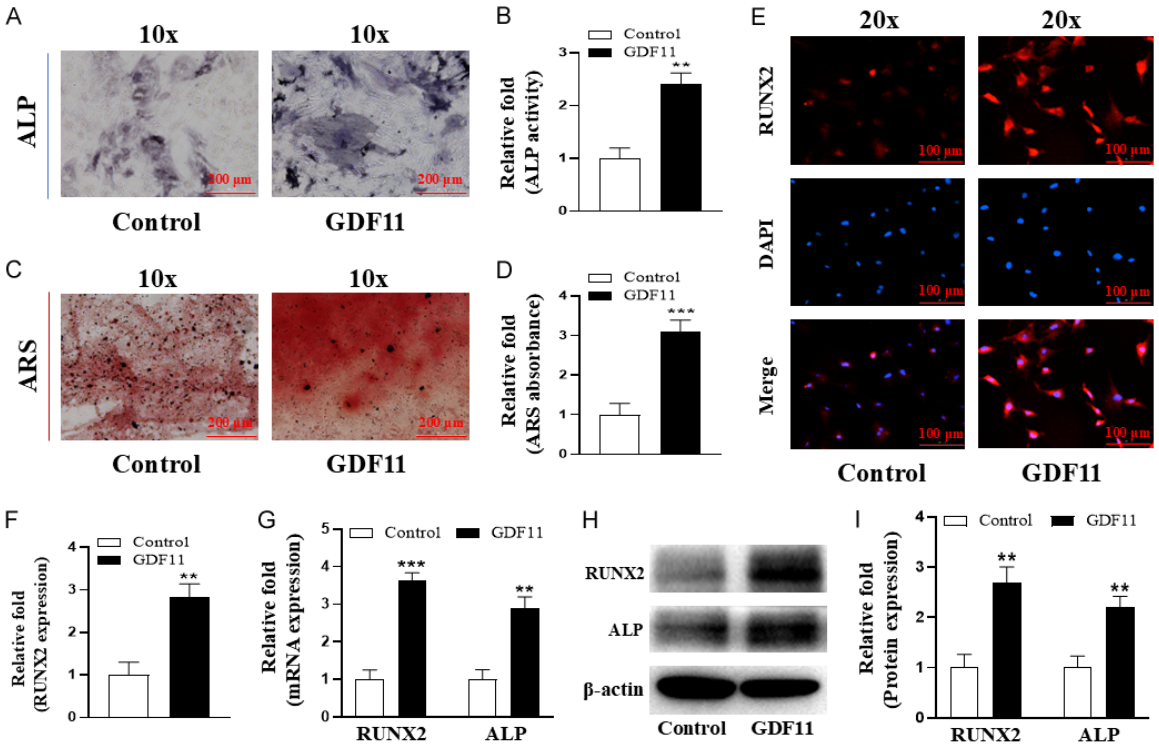

Figure 1. Osteogenic differentiation of rBMMSCs by GDF11. A. ALP staining on day 7 of osteoblast differentiation (scale bars = 200 μm); B. ALP activity on day 7 of osteoblast differentiation (scale bars = 200 μm); C. ARS on day 14 of osteoblast differentiation; D. Relative quantitative analysis of ARS; E, F. IF showing relative protein expression of RUNX2 on day 3 (Scale bars = 100 μm); G-I. Relative mRNA and protein expression of osteoblastogenic genes ALP and RUNX2 during osteoblast differentiation of rBMMSCs on day 3. (***P* < 0.01, ****P* < 0.001, vs. the control group. All experiments were performed in triplicate. All error bars are depicted as ± standard deviation).

Abcam), phospho-AMPK (p-AMPK; 1:1000, ab-133448, Abcam), total AMPK (t-AMPK; 1:1000, ab207442, Abcam), PINK1 (1:1000, ab186303, Abcam), and β-actin (1:3000, ab8226, Abcam) as a loading control. (3) After three 5-minute washes with TBST, membranes were incubated with horseradish peroxidase (HRP)-conjugated secondary antibody (1:5000, ZB-2306, ZSGB-BIO, Beijing, China) for 1 hour at room temperature. (4) Membranes were washed three additional times with TBST (5 minutes per wash).

Protein bands were visualized using a C-Digit Blot Scanner (LI-COR, USA) and quantified by densitometric analysis with ImageJ software (NIH, USA).

Statistical analysis

All data are presented as the mean ± standard deviation (SD). Statistical analyses were performed using GraphPad Prism software (version 8.0.2; GraphPad Software, USA). Comparisons between two groups were conducted using Student's t-test, while differences among multiple groups were evaluated using one-way analysis of variance (ANOVA). A *P* value of less than 0.05 was considered statistically significant.

Results

GDF11 promotes the osteogenic differentiation of rBMMSCs

To investigate the effect of GDF11 on osteogenic differentiation, rBMMSCs were treated with 10 ng/mL GDF11. The ALP staining on day 7 demonstrated that GDF11 significantly enhanced ALP expression in rBMMSCs, as evidenced by more intense staining and significantly increased ALP activity compared with the control group (**Figure 1A**, **1B**). Similarly, ARS staining performed on day 14 revealed a higher number of calcium nodules in the GDF11-treated group, indicating enhanced mineral deposition (**Figure 1C**, **1D**).

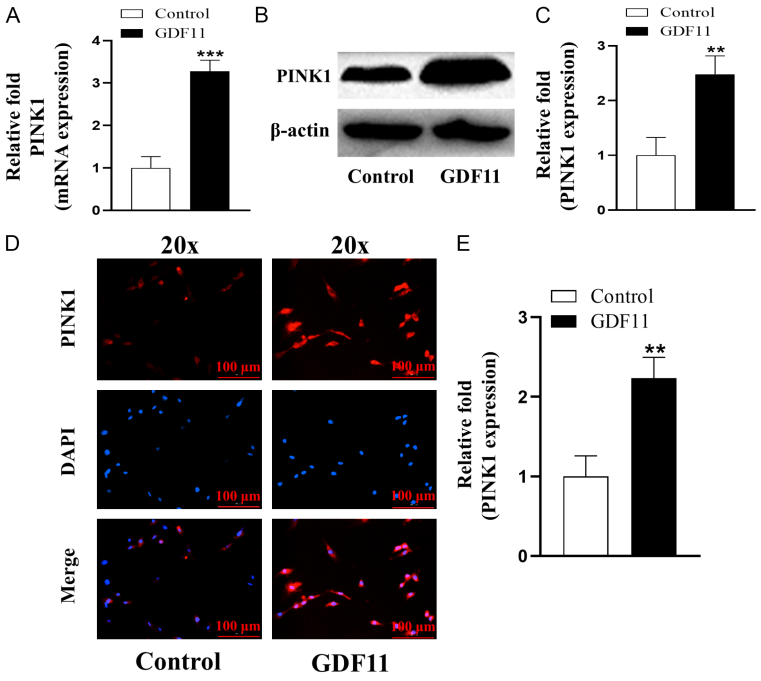

Figure 2. Mitophagy in rBMMSCs through GDF11. A. Relative mRNA expression of PINK1 on day 3; B, C. Relative protein expression of PINK1 on day 3; D, E. IF of relative protein expression of PINK1 on day 3 (scale bars = 100 μm. $^{**}P < 0.01$, $^{***}P < 0.001$, vs. the control group. All experiments were performed in triplicate. All error bars are depicted as ± standard deviation).

The expression levels of osteogenic marker genes were further analyzed to confirm these findings. Quantitative real-time PCR, western blotting, and immunofluorescence staining on day 3 showed that both *ALP* and *RUNX2* expression were significantly upregulated in the GDF11-treated cells relative to the control group (**Figure 1E-I**). These results demonstrate that GDF11 significantly promotes the osteogenic differentiation of rBMMSCs by enhancing ALP activity, mineralization, and the expression of genes associated with osteogenesis.

GDF11 promotes mitophagy in rBMMSCs

Mitophagy plays a crucial regulatory role in the osteogenic differentiation of BMMSCs by preserving mitochondrial integrity and modulating cellular energy metabolism and ROS balance. To investigate whether GDF11 influences Mitophagy in rBMMSCs, the expression of PINK1, a key marker of Mitophagy, was examined. Quantitative real-time PCR results showed that GDF11 stimulation significantly increased PINK1 mRNA expression compared with the control group (**Figure 2A**). Consistently, immunofluorescence and western blot analyses revealed a significant upregulation of PINK1 protein levels in GDF11-treated cells (**Figure 2B-D**).

These findings demonstrate that GDF11 promotes Mitophagy in rBMMSCs, suggesting that enhanced mitochondrial quality control may contribute to its pro-osteogenic effects.

Role of AMPK in GDF11-activated mitophagy in rBMMSCs

To elucidate the signaling pathway through which GDF11 regulates Mitophagy in rBMMSCs, AMPK phosphorylation levels were examined. Western blot analysis demonstrated that GDF11 treatment significantly increased AMPK phosphorylation, indicating activation of the AMPK signaling pathway (**Figure 3A**, **3B**). To further confirm the involvement of AMPK in GDF11-induced Mitophagy, rBMMSCs were treated with Compound C (10 μM), a specific AMPK inhibitor. Quantitative real-time PCR, western blotting, and immunofluorescence staining revealed that inhibition of AMPK by Compound C significantly reduced PINK1 expression and attenuated the mitophagy-promoting effect of GDF11 (**Figure 3C-G**).

These findings demonstrate that GDF11-induced Mitophagy in rBMMSCs is mediated through activation of the AMPK signaling pathway.

GDF11 promotes osteogenic differentiation of rBMMSCs via AMPK-dependent mitophagy

To investigate the role of Mitophagy in the osteogenic differentiation of rBMMSCs, AMPK-dependent mitophagy was inhibited using Compound C (10 μM). Following AMPK inhibition, a noticeable reduction in alkaline phosphatase (ALP) staining intensity and activity was observed. Moreover, the ability of GDF11 to enhance ALP production and enzymatic activity was significantly diminished (**Figure 4A**, **4B**). Similarly, ARS staining demonstrated that

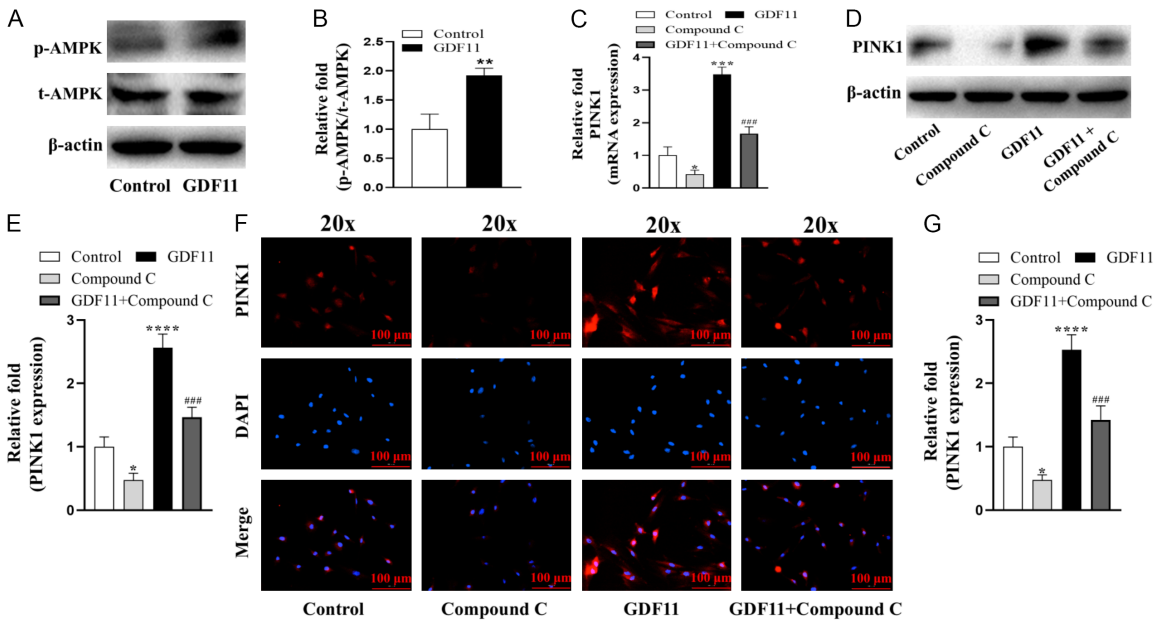

Figure 3. Role of AMPK in GDF11-activated Mitophagy in rBMMSCs. A, B. GDF11-induced changes in AMPK phosphorylation levels; C Relative mRNA expression of PINK1; D, E. Relative protein expression of PINK1; F, G. IF results of relative protein expression of PINK1 (scale bars = 100 μm. $^{**}P < 0.01$, $^{***}P < 0.001$, $^{****}P < 0.0001$, vs. the control group. $^{\#\#\#}P < 0.001$, vs. the GDF11 group. All experiments were performed in triplicate. All error bars are depicted as ± standard deviation).

Compound C significantly suppressed GDF11-induced calcium nodule formation (**Figure 4C**, **4D**).

Immunofluorescence analysis further revealed that inhibition of Mitophagy reduced RUNX2 expression, and the GDF11-mediated upregulation of RUNX2 was similarly abolished (**Figure 4E**, **4F**). In agreement with these observations, quantitative real-time PCR and western blot analyses showed that blocking AMPK-dependent mitophagy significantly attenuated the GDF11-induced increase in ALP and RUNX2 mRNA and protein expression on day 3 (**Figure 4G-I**).

These findings demonstrate that GDF11 promotes the osteogenic differentiation of rBMMSCs through activation of AMPK-dependent mitophagy.

Discussion

OP management challenges and the promise of BMMSC-targeted strategies

Despite significant progress in the management of OP, current therapeutic options remain limited by several challenges. Available pharmacological agents are costly and frequently associated with adverse effects, which contribute to poor patient adherence and reduced long-term efficacy [16]. Moreover, these treatments primarily focus on inhibiting bone resorption or transiently stimulating bone formation, without effectively restoring bone microarchitecture or addressing the underlying cellular pathology of OP.

The core pathogenic mechanism of OP involves dysfunction of BMMSCs, particularly mitochondrial impairment and diminished osteogenic differentiation potential. Mounting evidence indicates that BMMSCs derived from osteoporotic bone show defective mitochondrial biogenesis, premature senescence, and reduced mitophagy activity, collectively leading to excessive oxidative stress and compromised osteogenesis [17-19]. Current therapeutic strategies fail to correct these intrinsic metabolic deficiencies or rejuvenate the regenerative capacity of BMMSCs.

Therefore, targeting the rejuvenation of BMMSCs, primarily by restoring mitochondrial homeostasis through the enhancement of Mitophagy, represents a promising therapeutic direction. Such an approach could overcome the inherent differentiation blockade of osteoporotic BMMSCs and potentially achieve sustained bone

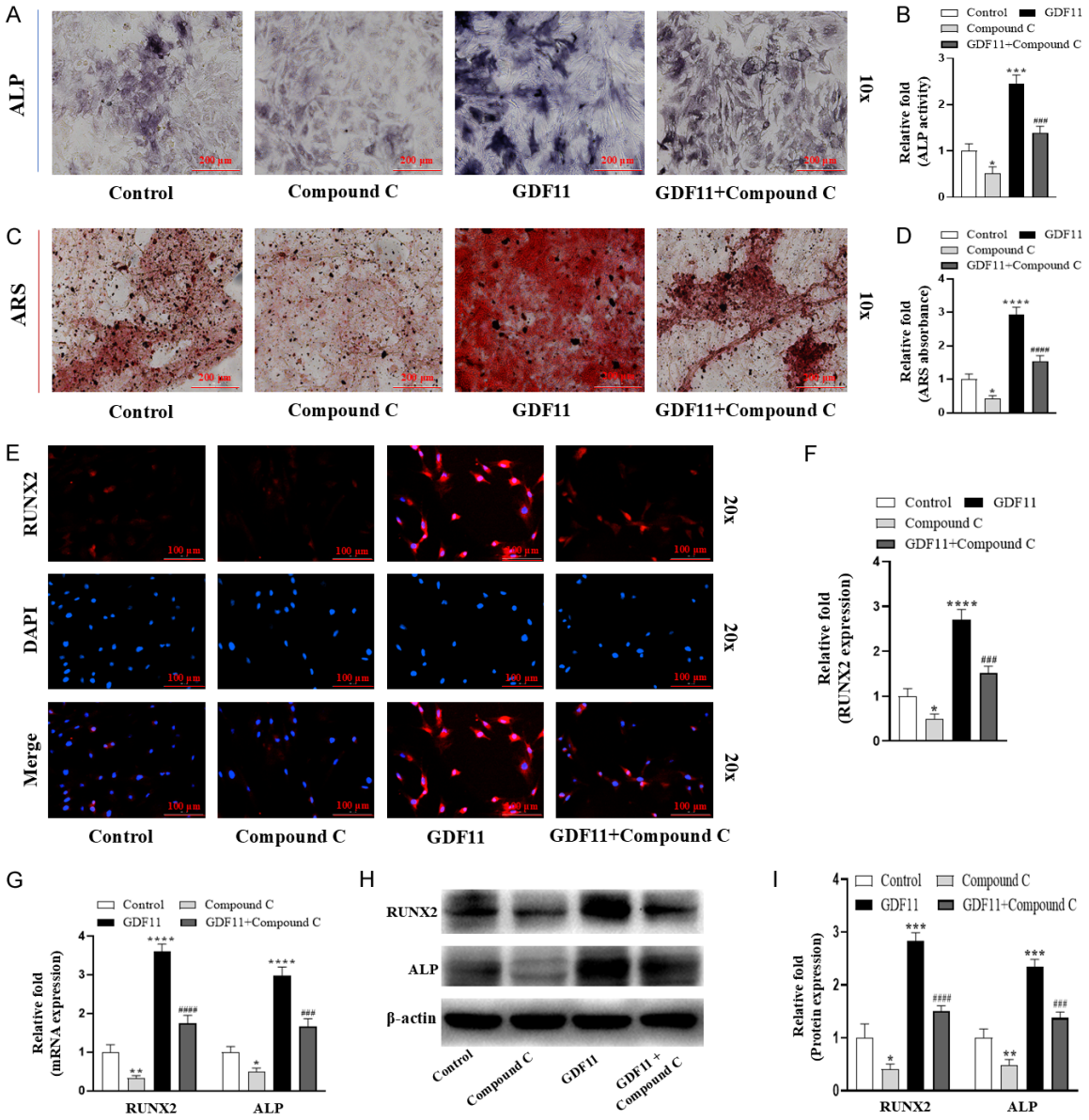

Figure 4. Osteogenic differentiation of rBMMSCs by GDF11 *via* AMPK-dependent Mitophagy. A. ALP staining on day 7 of osteoblast differentiation; B. ALP activity on day 7 of osteoblast differentiation; C. ARS on day 14 of osteoblast differentiation; D. Relative quantitative analysis of ARS; E, F. IF showing relative protein expression of RUNX2 on day 3; G-I. Relative mRNA and protein expression of osteogenic genes (*ALP* and *RUNX2*) during osteoblast differentiation of rBMMSCs on day 3 (scale bars = 100 μm. $^{*}P < 0.05$, $^{**}P < 0.01$, $^{***}P < 0.001$, $^{****}P < 0.0001$, vs. the control group. $^{\#\#\#}P < 0.001$, $^{\#\#\#}P < 0.0001$, vs. the GDF11 group. All experiments were performed in triplicate. All error bars are depicted as ± standard deviation).

regeneration, moving beyond the limitations of conventional treatments that only modulate bone turnover.

Mitophagy: a pivotal regulator of BMMSC function and OP pathogenesis

Mitophagy, the selective autophagic degradation of damaged mitochondria, plays a vital role in maintaining bone homeostasis and is critically implicated in the pathogenesis of OP and BMMSC dysfunction. During the osteogenic differentiation of BMMSCs, extensive metabolic and structural reprogramming occurs to meet high energy demands, which are tightly regulated by multiple signaling pathways. Mitophagy ensures mitochondrial quality control by remov-

ing dysfunctional mitochondria, maintaining low levels of ROS and sufficient ATP production, both essential for proper osteogenic differentiation [20]. This process is primarily mediated through the PINK1-Parkin axis and the AMPK-ULK1 signaling pathway, which target depolarized mitochondria for lysosomal degradation.

Impaired Mitophagy disrupts cellular metabolic homeostasis and contributes directly to the progression of OP. When Mitophagy is compromised, damaged mitochondria accumulate, leading to excessive ROS production and oxidative stress. Elevated ROS oxidizes and inactivates key transcription factors, including RUNX2, hindering its nuclear translocation and suppressing osteogenic gene expression [21]. High ROS levels also damage proteins, lipids, and DNA, further impairing the signalling networks required for differentiation. The persistence of dysfunctional mitochondria disrupts ATP synthesis, leading to an energy deficit that fails to support the metabolically demanding process of osteogenic differentiation. As a result, the synthesis of osteogenesis-related enzymes and matrix proteins declines, mineralization is reduced, and the differentiation process may be prematurely arrested [22].

Clinical and experimental evidence further supports the link between mitophagy dysfunction and impaired bone formation, also known as osteogenesis. Decreased expression of mitophagy markers such as PINK1 and LC3 II/I has been observed in BMMSCs isolated from postmenopausal women and ovariectomized animal models of OP [23]. Moreover, genetic studies have demonstrated causality: PINK1 overexpression restores Mitophagy and osteogenic differentiation in OP-BMMSCs, whereas PINK1 deletion recapitulates osteoporotic phenotypes [24]. Damaged mitochondria also exhibit reduced membrane potential and increased permeability, leading to the release of cytochrome c into the cytoplasm. This, in turn, activates the caspase cascade and induces apoptosis, decreasing the BMMSC population and impairing osteoblast formation.

In this study, the role of mitochondrial quality control in the osteogenic differentiation of rBMMSCs was confirmed. Our findings demonstrate that Mitophagy in these cells is mediated by AMPK signaling. Inhibition of AMPK phosphorylation using Compound C resulted in mitochondrial dysfunction, reduced PINK1 expression, and suppression of osteogenic marker genes, leading to a significant decline in osteogenic capacity. Activation of Mitophagy by GDF11 significantly enhanced osteogenic differentiation, supporting the notion that GDF11 exerts its pro-osteogenic effects through the AMPK–mitophagy axis. These results highlight the crucial role of mitochondrial homeostasis in preserving the osteogenic potential of BMMSCs.

GDF11: a potential regulator of mitophagy and mitochondrial health

The GDF11, a member of the transforming growth factor-β (TGF-β) superfamily, has garnered considerable attention for its potential rejuvenating properties, particularly in the context of age-related degeneration. Declining GDF11 levels have been associated with aging phenotypes characterized by mitochondrial dysfunction, suggesting that GDF11 may contribute to the preservation of mitochondrial integrity, possibly through the regulation of Mitophagy [25]. GDF11 is believed to signal through activin receptor-like kinase (Alk) receptors, primarily Alk4, Alk5, and Alk7, leading to activation of downstream SMAD2/3 pathways, which in turn may regulate the transcription of key mitophagy-associated genes such as PINK1, Parkin, BNIP3, NIX, and FUNDC1, or modulate upstream energy sensors including AMPK [26].

In addition to its role in Mitophagy, GDF11 has been reported to enhance mitochondrial biogenesis and function [27], both of which are tightly coordinated with Mitophagy to maintain a healthy mitochondrial network. Restoration of physiological GDF11 levels in aged models has been shown to improve mitochondrial quality and reduce oxidative stress markers [28], effects that are likely mediated, at least in part, by augmented Mitophagy. However, direct mechanistic evidence defining GDF11 as a key regulator of mitophagy initiation or flux, identifying specific receptor complexes, and delineating downstream signaling events remains limited [29]. Moreover, the role of GDF11 in modulating osteogenic differentiation of BMMSCs in the context of OP has not been fully elucidated.

The results demonstrated that GDF11 activates the AMPK signaling pathway and pro-

motes AMPK phosphorylation in rBMMSCs. Activated AMPK drives Mitophagy, improving mitochondrial function and facilitating osteogenic differentiation. Inhibition of AMPK-mediated Mitophagy using Compound C significantly impaired the osteogenic potential of rBMMSCs and reduced the expression of genes related to osteogenesis. GDF11 was able to partially restore Mitophagy and reverse the suppression of osteogenic differentiation even under conditions of inhibited AMPK phosphorylation.

These findings highlight a critical role for GDF11 in promoting osteogenic differentiation of rBMMSCs through the activation of AMPK-dependent mitophagy. This mechanism provides new insight into how GDF11 contributes to mitochondrial quality control and bone regeneration, underscoring its potential as a therapeutic target for the treatment of osteoporosis.

Our key finding: GDF11 rejuvenates OP-BMMSCs via AMPK-dependent mitophagy

To the best of our knowledge, this study provides the first direct evidence that GDF11 promotes the osteogenic differentiation of rBMMSCs through activation of AMPK-dependent mitophagy. GDF11 treatment significantly increased AMPK phosphorylation, whereas pharmacological inhibition of AMPK with Compound C abrogated GDF11-induced Mitophagy and osteogenesis, confirming that AMPK activation is essential for GDF11's biological effects. Furthermore, GDF11 upregulated the expression of key mitophagy markers such as PINK1. At the same time, blockade of Mitophagy attenuated its pro-osteogenic activity, establishing a clear mechanistic link between mitochondrial quality control and osteoblast lineage commitment.

Our findings reveal that GDF11 effectively overcomes the accumulation of damaged mitochondria and oxidative stress in osteoporotic BMMSCs, factors known to inhibit RUNX2 activity, by promoting AMPK-driven mitophagy, restoring the expression of osteogenic genes. These results demonstrate that GDF11 rescues mitophagy dysfunction in osteoporotic BMMSCs by activating AMPK, reversing mitochondrial impairment, and reinstating their osteogenic potential.

This mechanism represents a paradigm shift from conventional osteoporosis therapies that primarily target the balance between bone resorption and formation. By directly modulating the metabolic and mitochondrial foundation of skeletal regeneration, GDF11-mediated activation of Mitophagy emerges as a pivotal regulatory switch governing bone anabolism, representing a promising therapeutic avenue for osteoporosis.

Limitations and future directions

While the present findings underscore the therapeutic promise of GDF11, several important questions remain to be addressed. The reported age-dependent variations in circulating GDF11 levels, along with the ongoing debate regarding its tissue-specific functions, warrant further investigation, particularly within the context of age-related osteoporosis. Moreover, the development of optimized delivery systems, such as hydrogel-based GDF11 scaffolds, and the comprehensive evaluation of their long-term efficacy and safety are critical next steps toward successful clinical translation.

Conclusions

This study identifies a previously unrecognized mechanistic pathway by which GDF11 promotes the osteogenic differentiation of BMMSCs through the activation of AMPK-mediated Mitophagy, restoring mitochondrial function impaired in osteoporosis. The elucidated "GDF11-AMPK-mitophagy-osteogenesis" axis represents a novel therapeutic target for the development of anabolic strategies aimed at enhancing bone formation through the rejuvenation of stem cell function.

Acknowledgements

This work was supported by Natural Science Foundation of Hubei Province (grant no JCZRQN202501242) and Wuhan Natural Science Foundation (grant no 202502070-1020269).

Disclosure of conflict of interest

The authors declare that the research was conducted in the absence of any commercial or financial relationships that could be construed as a potential conflict of interest.

Address correspondence to: Kai Xiao, Department of Orthopedic Surgery, Wuhan Fourth Hospital, 473 Hanzheng Street, Qiaokou District, Wuhan 430030, Hubei, China. E-mail: 1785160035@qq.com

References

[1] De Martinis M, Sirufo MM, Polsinelli M, Placidi G, Di Silvestre D and Ginaldi L. Gender differences in Osteoporosis: a single-center observational study. World J Mens Health 2021; 39: 750-759.

[2] Kanis JA, Cooper C, Rizzoli R and Reginster JY; Scientific Advisory Board of the European Society for Clinical and Economic Aspects of Osteoporosis (ESCEO) and the Committees of Scientific Advisors and National Societies of the International Osteoporosis Foundation (IOF). European guidance for the diagnosis and management of Osteoporosis in postmenopausal women. Osteoporos Int 2019; 30: 3-44.

[3] Compston JE, McClung MR and Leslie WD. Osteoporosis. Lancet 2019; 393: 364-376.

[4] Kim MS, Chung HJ and Kim KI. Optimal concentration of mesenchymal stem cells for fracture healing in a rat model with long bone fracture. World J Stem Cells 2022; 14: 839-850.

[5] Cheng YH, Liu SF, Dong JC and Bian Q. Transcriptomic alterations underline aging of osteogenic bone marrow stromal cells. World J Stem Cells 2021; 13: 128-138.

[6] Döhla J, Kuuluvainen E, Gebert N, Amaral A, Englund JI, Gopalakrishnan S, Konovalova S, Nieminen AI, Salminen ES, Torregrosa Muñumer R, Ahlqvist K, Yang Y, Bui H, Otonkoski T, Käkelä R, Hietakangas V, Tyynismaa H, Ori A and Katajisto P. Metabolic determination of cell fate through selective inheritance of mitochondria. Nat Cell Biol 2022; 24: 148-154.

[7] Palikaras K, Lionaki E and Tavernarakis N. Mechanisms of mitophagy in cellular homeostasis, physiology and pathology. Nat Cell Biol 2018; 20: 1013-1022.

[8] Chen CT, Shih YR, Kuo TK, Lee OK and Wei YH. Coordinated changes of mitochondrial biogenesis and antioxidant enzymes during osteogenic differentiation of human mesenchymal stem cells. Stem Cells 2008; 26: 960-8.

[9] Loffredo FS, Steinhauser ML, Jay SM, Gannon J, Pancoast JR, Yalamanchi P, Sinha M, Dall'Osso C, Khong D, Shadrach JL, Miller CM, Singer BS, Stewart A, Psychogios N, Gerszten RE, Hartigan AJ, Kim MJ, Serwold T, Wagers AJ and Lee RT. GDF11 is a circulating factor that reverses age-related cardiac hypertrophy. Cell 2013; 153: 828-39.

[10] Qi X, Xiao Q, Sheng R, Jiang S, Yuan Q and Liu W. Endogenous GDF11 regulates odontogenic differentiation of dental pulp stem cells. J Cell Mol Med 2020; 24: 11457-11464.

[11] Suh J, Kim NK, Lee SH, Eom JH, Lee Y, Park JC, Woo KM, Baek JH, Kim JE, Ryoo HM, Lee SJ and Lee YS. GDF11 promotes osteogenesis as opposed to MSTN, and follistatin, a MSTN/GDF11 inhibitor, increases muscle mass but weakens bone. Proc Natl Acad Sci U S A 2020; 117: 4910-4920.

[12] Toyama EQ, Herzig S, Courchet J, Lewis TL Jr, Losón OC, Hellberg K, Young NP, Chen H, Polleux F, Chan DC and Shaw RJ. Metabolism. AMP-activated protein kinase mediates mitochondrial fission in response to energy stress. Science 2016; 351: 275-281.

[13] Herzig S and Shaw RJ. AMPK: guardian of metabolism and mitochondrial homeostasis. Nat Rev Mol Cell Biol 2018; 19: 121-135.

[14] Yang W, Qiu C, Lv H, Zhang Z, Yao T, Huang L, Wu G, Zhang X, Chen J and He Y. Sirt3 protects retinal pigment epithelial cells from high glucose-induced injury by promoting mitophagy through the AMPK/mTOR/ULK1 pathway. Transl Vis Sci Technol 2024; 13: 19.

[15] Xu Y, Hu X, Li F, Zhang H, Lou J, Wang X, Wang H, Yin L, Ni W, Kong J, Wang X, Li Y, Zhou K and Xu H. GDF-11 protects the traumatically injured spinal cord by suppressing pyroptosis and necroptosis via TFE3-mediated autophagy augmentation. Oxid Med Cell Longev 2021; 2021: 8186877.

[16] Stelea CG, Bologa E, Boişteanu O, Platon AL, Stelea ŞO, Geleşu GL, Onică CA, Şulea D, Ciofu ML and Costan VV. Bisphosphonate-related osteonecrosis of the jaw: a 10-year analysis of risk factors and clinical outcomes. J Clin Med 2025; 14: 4445.

[17] Duan S, Zhang Q, Zhu J and Wang J. SS-31 targets NOS2 to enhance osteogenic differentiation in aged BMMSCs by restoring mitochondrial function. Organogenesis 2025; 21: 2519649.

[18] Liu F, Yuan L, Li L, Yang J, Liu J, Chen Y, Zhang J, Lu Y, Yuan Y and Cheng J. S-sulfhydration of SIRT3 combats BMMSC senescence and ameliorates OP via stabilizing heterochromatic and mitochondrial homeostasis. Pharmacol Res 2023; 192: 106788.

[19] Sikora M, Śmieszek A, Pielok A and Marycz K. MiR-21-5p regulates the dynamic of mitochondria network and rejuvenates the senile phenotype of bone marrow stromal cells (BMMSCs) isolated from osteoporotic SAM/P6 mice. Stem Cell Res Ther 2023; 14: 54.

[20] Shi J, Wen J and Hu L. 17β-estradiol promotes osteogenic differentiation of BMMSCs by regulating mitophagy through ARC. J Orthop Surg Res 2025; 20: 35.

[21] Lee SY, An HJ, Kim JM, Sung MJ, Kim DK, Kim HK, Oh J, Jeong HY, Lee YH, Yang T, Kim JH, Lim HJ and Lee S. PINK1 deficiency impairs osteoblast differentiation through aberrant mitochondrial homeostasis. Stem Cell Res Ther 2021; 12: 589.

[22] Cheng H, Feng JM, Figueiredo ML, Zhang H, Nelson PL, Marigo V and Beck A. Transient receptor potential melastatin type 7 channel is critical for the survival of bone marrow derived mesenchymal stem cells. Stem Cells Dev 2010; 19: 1393-403.

[23] Chen XJ, Yang YY, Pan ZC, Xu JZ, Jiang T, Zhang LL, Zhu KC, Zhang D, Song JX, Sheng CX, Sun LH, Tao B, Liu JM and Zhao HY. The inhibition of PINK1/Drp1-mediated mitophagy by hyperglycemia leads to impaired osteoblastogenesis in diabetes. iScience 2024; 28: 111519.

[24] Yuan J, Gao YS, Liu DL, Pang Tai AC, Zhou H, Papadimitriou JM, Zhang CQ, Zheng MH and Gao JJ. PINK1-mediated mitophagy contributes to glucocorticoid-induced cathepsin K production in osteocytes. J Orthop Translat 2022; 38: 229-240.

[25] Zhang P, Zhai H, Zhang S, Ma X, Gong A, Xu Z, Zhao W, Song H, Li S, Zheng T, Ying Z, Cheng L, Zhao Y and Zhang L. GDF11 protects against mitochondrial-dysfunction-dependent NLRP3 inflammasome activation to attenuate osteoarthritis. J Adv Res 2025; 73: 501-515.

[26] Jiao L, Shao Y, Yu Q, Li M, Wang Y, Gong M, Yang X, Liu T, Li Z, Liu H, Zhang Y, Tan Z, Sun L, Xuan L, Yin H, Zhang Y, Cai B, Zhang Y and Yang B. GDF11 replenishment protects against hypoxia-mediated apoptosis in cardiomyocytes by regulating autophagy. Eur J Pharmacol 2020; 885: 173495.

[27] Chen L, Luo G, Liu Y, Lin H, Zheng C, Xie D, Zhu Y, Chen L, Huang X, Hu D, Xie J, Chen Z, Liao W, Bin J, Wang Q and Liao Y. GDF11 attenuates cardiac ischemia reperfusion injury via enhancing mitochondrial biogenesis and telomerase activity. Cell Death Dis 2021; 12: 665.

[28] Tao P, Zhang HF, Zhou P, Wang YL, Tan YZ and Wang HJ. Growth differentiation factor 11 alleviates oxidative stress-induced senescence of endothelial progenitor cells via activating autophagy. Stem Cell Res Ther 2024; 15: 370.

[29] Andrianova NV, Zorova LD, Pevzner IB, Kolosova NG, Plotnikov EY and Zorov DB. Calorie restriction provides kidney ischemic tolerance in senescence-accelerated OXYS rats. Int J Mol Sci 2022; 23: 15224.